Optical forming analysis of the preforming process

F. Zacharias, M. Zerwer, S. Rasche,
Institute of Composite Structures and Adaptive Systems, Composite Process Technology,
Ottenbecker Damm 12, 21684 Stade, Germany

Abstract

The preforming of carbon fiber semi-finished parts is responsible for a major share of the total costs at RTM processes. In order to identify the areas with the highest degree of deformation, an optical forming analysis was used. One requirement for this measurement technique is the application of a regular grid of red dots. Therefore different methods for the application have been investigated and automated. Furthermore the integration of the optical camera into the process has been achieved. As a result the measuring process could be automated. In a final step the measuring technology was validated at the automated preforming process of an aircraft fuselage frame segment.

1. INTRODUCTION

Improving the preforming process not using “trial and error” methods requires quality assurance measurements to determine elongations, the topology and so forth. When those systems can be implemented, complex forming problems can be analyzed and reality can be compared with results of draping simulations.

The challenge to use those systems is the application of a regular grid of red dots on a carbon fiber semi-finished product.

The airframe can be seen in Figure 1. Basically it is a curved part with two curvatures. The cross-section has a “z” shape. The preform consists of triaxial and biaxial non crimped fabrics (ncf) plies which need to be draped over a double curvature tool. The frame also consists of single curved UD-patches.

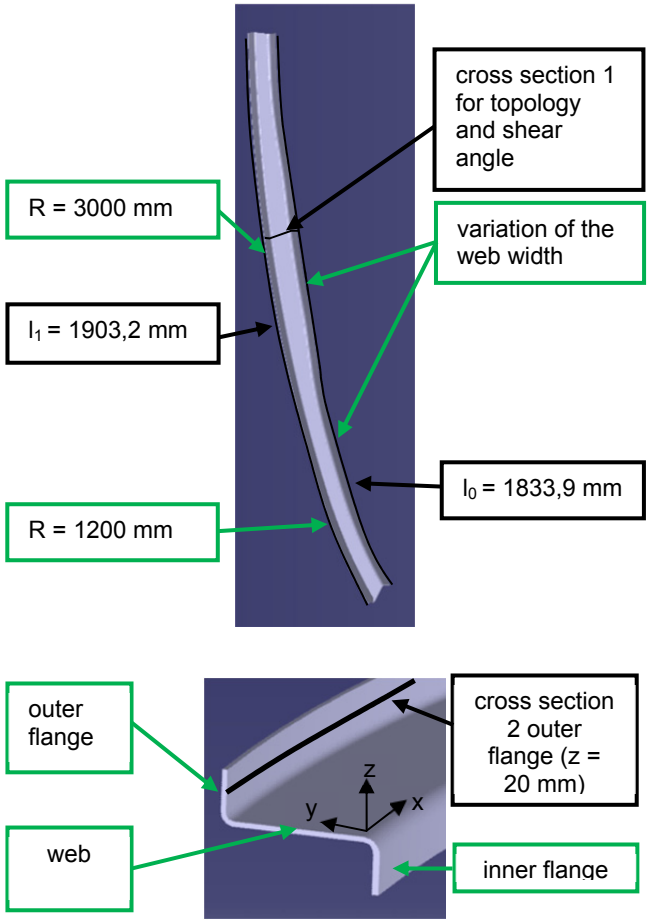

Figure 1: shape of frame with “z”cross-section

2. THE RTM PROCESS AT DLR STADE

At the DLR site in Stade (Germany) an automated RTM process chain has been build up [1]. The preforming consists of multiple steps, which can be seen in Figure 2. In *step 1* a 2D-ply is provided by the material supply. In *step 2* this ply is picked up by a robot and draped into a three-dimensional shape, by a custom-made end-effector (Figure 5). To fix the plies to the tool after draping the corresponding draping tool is equipped with vacuum-capability.

In order to fix the plies and smaller patches to each other the binder on the carbon fiber is locally activated by using the process of electrical resistance heating in *step 3*. During this process the preform is compacted between electrode and tool, while an electrical current is applied. Because of the high electrical resistance of the carbon fibers, heat is generated [2]. In *step 4* the preform is transported from the draping tool to the consolidation tool, which has no integrated vacuum. In *step 5* the preform gets consolidated. For the consolidation pressures up to 4e5 Pa and temperatures up to 150°C through infrared radiation are applied.

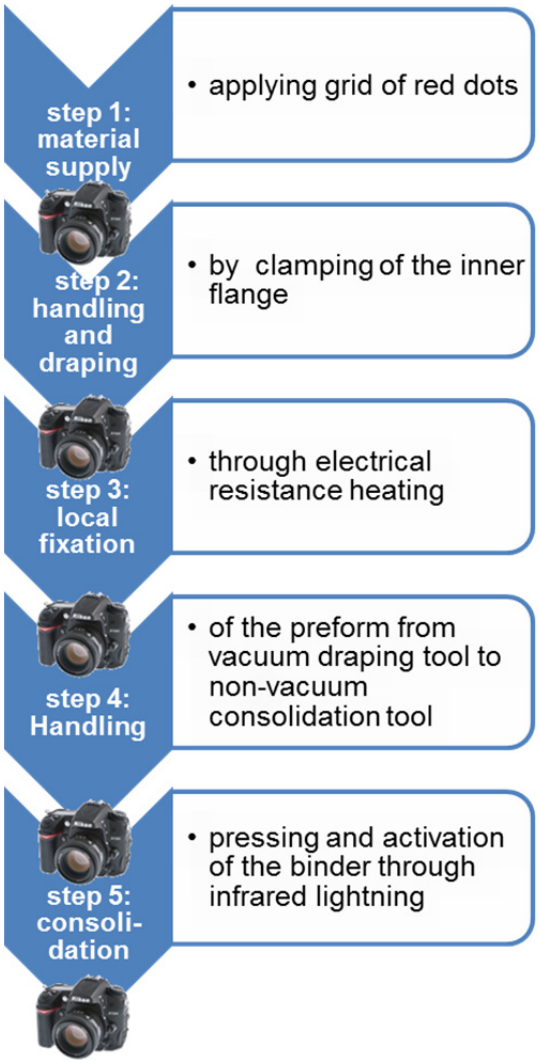

Figure 2: preforming process

For the experiments a bidirectional ncf (V2-010-PB1-005-IMS65 E23 24k-BD1-0388-1270) of the company Toho Tenax was used.

3. THEORETICAL MODEL

As a hypothesis it is stated that a rectangular ply is stretched on one side from l_0 to l_1 in order to get the flattened frame shape, which looks like a circular segment. This is illustrated in Figure 3. Note that the local coordinate system follows the curvature.

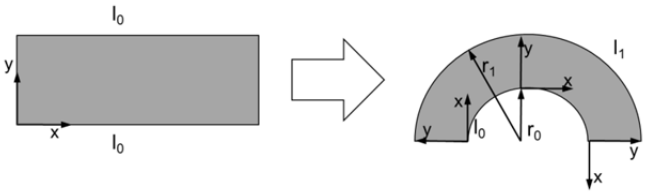

Figure 3: Preforming model of curved frames

During the draping the material in the area of the outer flange needs to be stretched from l_0 = 1833,9 mm to l_1=1903,2 mm. So the theoretical elongation can be calculated by formula (1):

$$\varepsilon_{x_{theoretical}} = \frac{r_1 - r_0}{r_1} \cdot 100\% = \frac{l_1 - l_0}{l_1} \cdot 100\% = \frac{1903{,}2\ mm - 1833{,}9\ mm}{1903{,}2\ mm} \cdot 100\% \approx 3{,}6\ \% \quad (1)$$

The semi-finished products are stretched from (1) to (2), which is illustrated in Figure 4. The length of the carbon fiber *b* stays the same and therefore the fiber angle $\varphi(r_1)$ is changing as well and can be calculated as shown in formula (2).

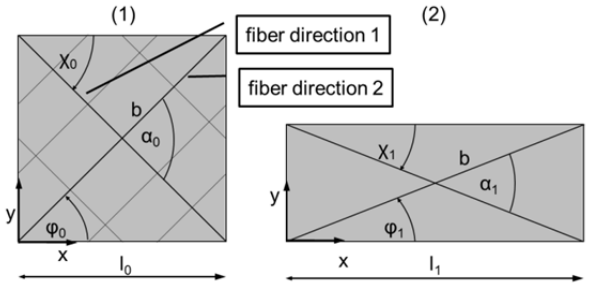

Figure 4: correlation of elongation and fiber angle [3]

$$\varphi_1(r_1) = \cos^{-1}\left(\cos\varphi_0 \cdot \frac{r_1}{r_0}\right) = \cos^{-1}\left(\cos\varphi_0 \cdot \frac{l_1}{l_0}\right) = \cos^{-1}\left(\cos(45°) \cdot \frac{1903{,}2\ mm}{1833{,}9\ mm}\right) = 42{,}79° \quad (2)$$

Since a biaxial ncf was investigated it is assumed that each layer will behave the same ($\varphi_0 - \varphi_1 = \chi_0 - \chi_1$). The shear angle is defined as the difference between the angle between the fiber orientations. As a result there is a correlation between the shear angle $\gamma_{theoretical}$ and the fiber angle $\rho_1(r)$, which can be seen in formula (3).

$$\gamma_{theoretical} = \alpha_0 - \alpha_1 = 2 \cdot (\rho_0 - \rho_1(r)) = 2 \cdot (45° - 42{,}79°) = 4{,}42° \quad (3)$$

By combining formula (2) and formula (3) the shear angle $\gamma_{theoretical}$ can be calculated as a function of the radius r_1.

$$\gamma_{theoretical}(r_1) = 2 \cdot (\rho_0 - \cos^{-1}\left(\cos\varphi_0 \cdot \frac{r_1}{r_0}\right)) \quad (4)$$

4. OPTICAL FORMING ANALYSIS

The optical forming analysis was originally used in the process of metal sheet forming. Later works showed that this measurement system can be equally used to analyze the forming behavior of ncf's and woven fabrics [4]. For this measurement the system ARGUS of the company GOM is used. The following steps are necessary to perform a measurement (see Figure 2)

1. Applying a regular grid of dots
2. Taking 1st set of pictures from at least 3 different views
3. Forming of the specimen
4. Taking 2nd set of pictures from at least 3 different views

The information for major strain, minor strain, elongation etc. is gathered by comparing the grid before and after draping. Additionally the topology of the preform can be measured and compared with a 3D-model.

In order to obtain a robust and reproducible measurement the camera was attached to an end-effector (Figure 5). To conduct a measurement the robot moves to previously teached positions and triggers the camera at each position to capture a picture. As a result the measurement could be automated and the distance between camera and sample is always the same, which is important since the camera has a fixed distance where it is focused.

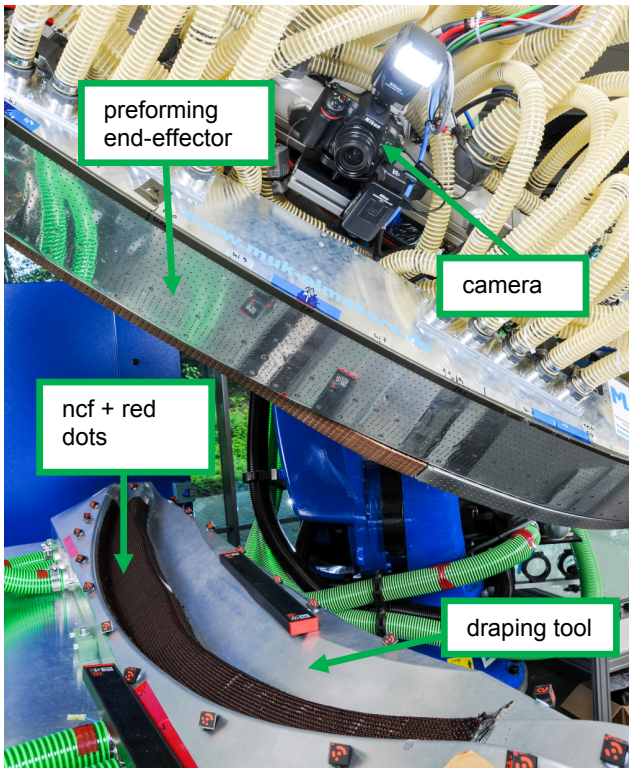

Figure 5: Handling and preforming end-effector with camera

5. APPLYING A GRID ON THE NCF

In order to find an automated and reliable way to apply a regular grid to the ncf, different ways to generate the grid were investigated. The results are displayed in Figure 6.

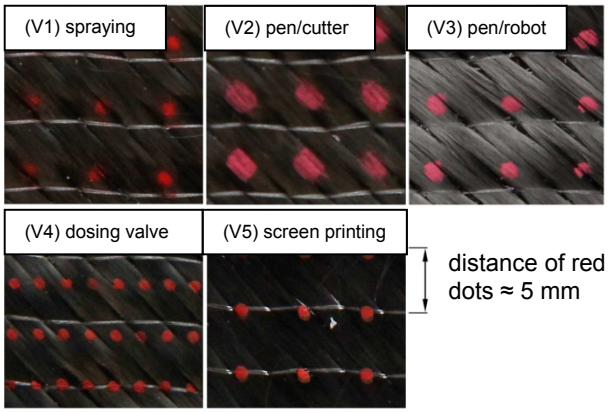

Figure 6: Different methods to apply a regular grid of red dots [3]

In terms of size, sharpness and robustness the dots applied by dosing valve and by screen printing performed best. Since the dosing valve could be easily integrated into the existing infrastructure this method was chosen.

6. DRAPING

Rectangular biaxial cuttings need to be draped into the right shape. The elongation in the direction of the frame can be seen in Figure 7. It can be observed, that the elongation in frame direction is not equally distributed. Mainly in the area of smaller radius the elongation is higher. Furthermore the deformation is significant in the outer flange and the web, whereas in the inner flange there is no elongation. At the beginning and at the end the elongation is near zero, which can be explained by the edge effect.

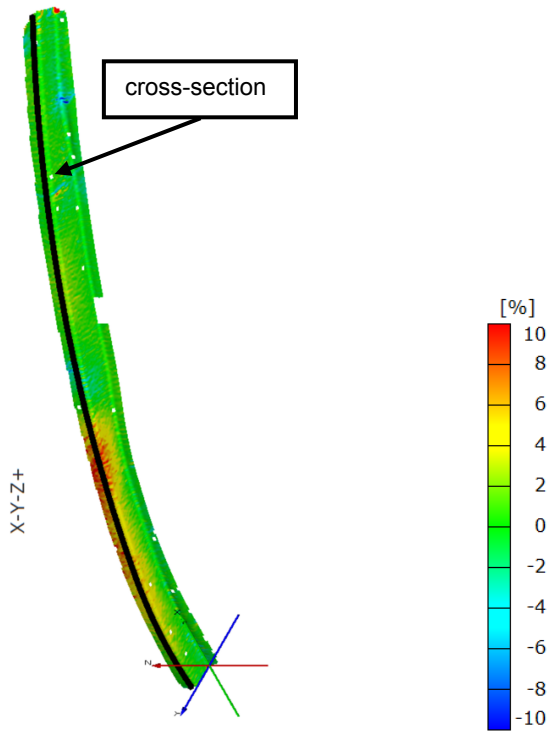

Figure 7: Elongation in frame direction ε_x after draping of biaxial cutting (step 2)

In Figure 8 the elongation ε_y in radial direction of the frame is shown. The most shortening is in the same area where the elongation in frame direction ε_x is the highest. Also in this figure, nearly no elongation can be measured at the border area.

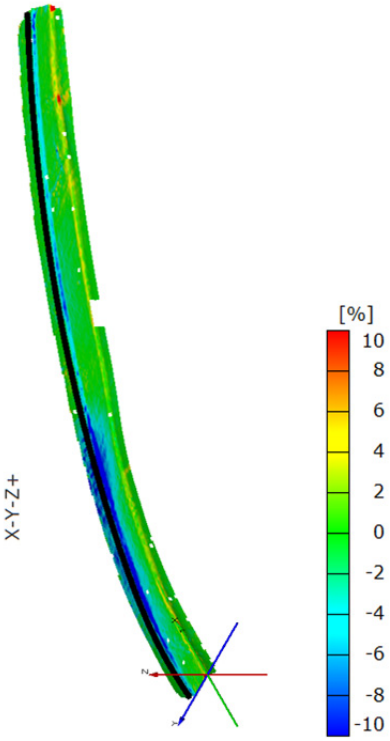

Figure 8: Elongation in radial direction ε_y after draping (step 2)

The shear angle is displayed in Figure 9. The highest values ($\gamma_{max,real} > 15°$) can be found in the inner radius right at the curvature change. In reality places with a high shear angle gradient are potential wrinkles spots.

The average shear angle over the frame arc length is $\gamma_{mean,real} = 2{,}64°$ after preforming (step 2). The theoretical shear angle of $\gamma_{theoretical} = 4{,}4°$ is around 66 % bigger.

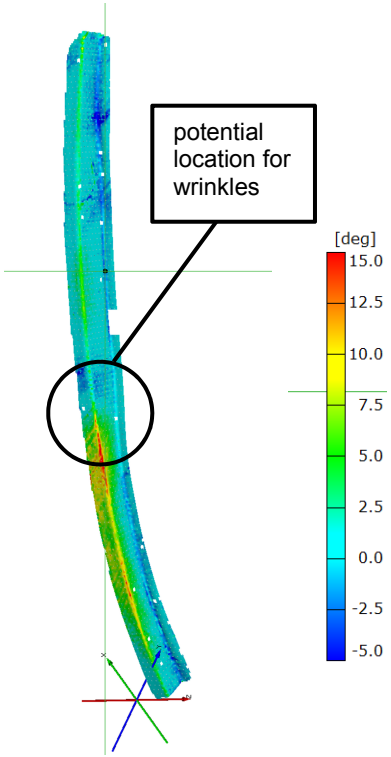

Figure 9: shear angle γ after draping (step 2)

It can be observed, that high shear angles γ go hand in hand with higher values for elongation in frame direction ε_x. Formula (3) and (4) show the correlation between the shear angle and fiber orientation. In Figure 10 the measured and the calculated shear angels are plotted over the cross section 1 marked in Figure 1. This model is predicting higher shear angles compared to the measured shear angles.

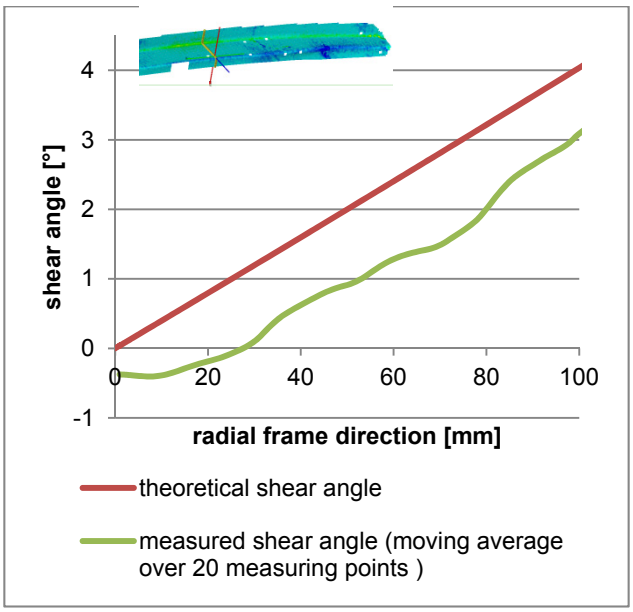

Figure 10: theoretical and measured shear angle over cross section 1

In Figure 11 the distance between the upper side of the preformed ncf and the tool surface is displayed. The preform and tool surface were overlapped by best fit. The maximum distance was 3 mm. Even small distances are visible like the pocket of the preforming tool, which is 1,1 mm deep.

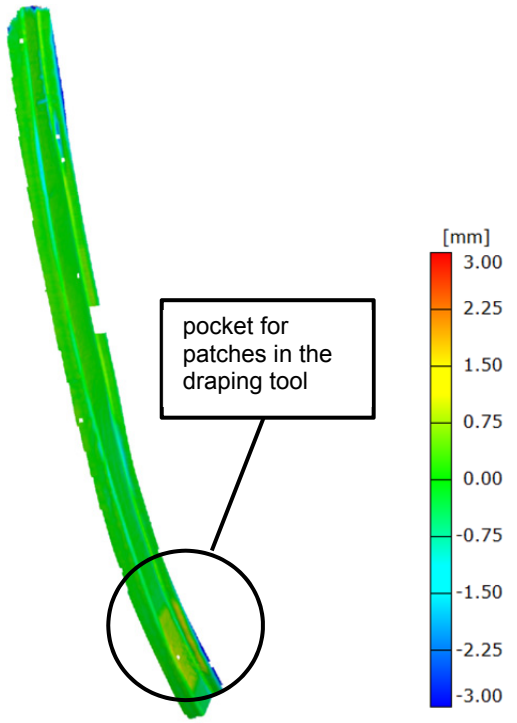

Figure 11: distance between preform and tool after preforming (step 2)

7. BINDER ACTIVATION, CONSOLIDATION AND HANDLING

In Figure 12 one can see the elongation in frame-direction ε_x over the cross-section 2. The position of the cross-section 2 in the outer flange is shown in Figure 1. The elongation in x-direction was plotted after the process steps draping, binder activation, handling and consolidation.

The green line in Figure 12 shows the elongation after *draping (step 2)*. The biaxial NCF is stretched up to 8 % in x-direction (in average 2,4 %) during the draping step. In the area of the large radius the elongation ε_x is with around 1 % rather small. A small area where the curvature is changing shows a compression of about 1 %.

After the process of *binder activation (step 3)* the preform seemed to have moved on the tool in x-direction. The reason might be the electrode which was not fully aligned rectangular to the tool.

During the next process step *handling (step 4)* of the preform to the consolidation tool (no suction capability) the preformed ply relaxed towards its original state. Therefore the average elongation in x-direction declines to about 1,5 %.

After the *consolidation process (step 5)* the average elongation in x-direction declines further down to 1,4%.

The average elongation ε_x after each preforming step and the theoretical elongation from Equation 3 are shown in Figure 13.

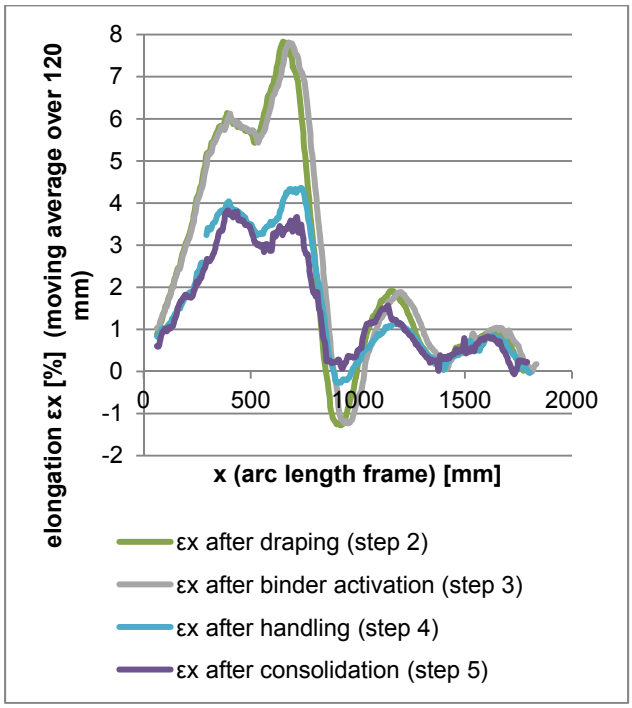

Figure 12: elongation in frame direction in the outer flange ε_x plotted over black line displayed in Figure 7

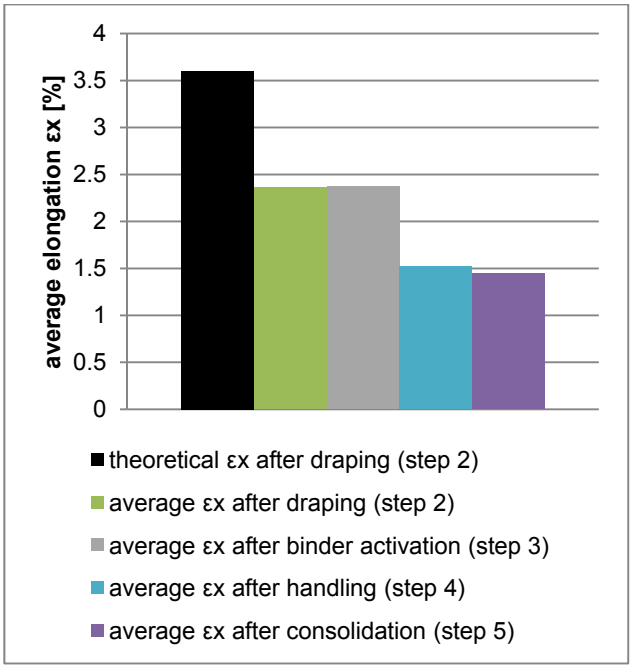

Figure 13: average elongation ε_x after different preforming steps

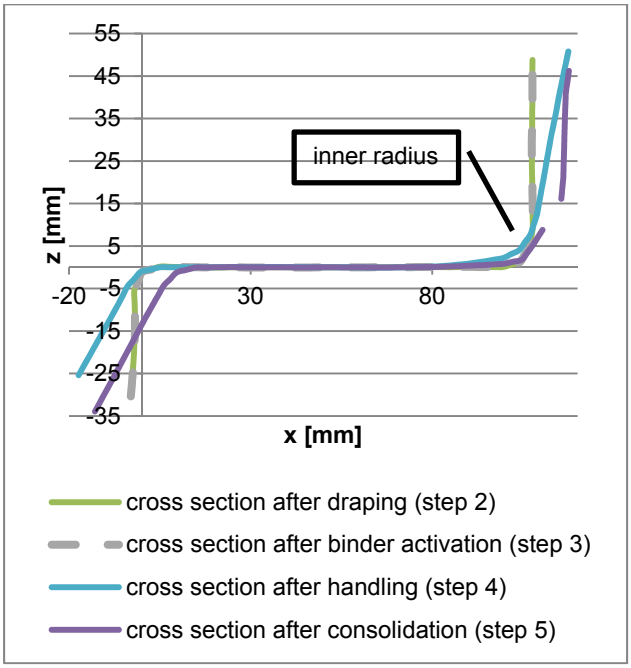

Figure 14: topology cross section after different preforming steps

The topology of the frame cross section 1 of Figure 1 after each preforming step is plotted in Figure 14. The position of the cross-section for the topology is marked in Figure 1. After the *preforming (step 2)* the preform has nearly an ideal z-cross-section, since it is fixed by airflow to the draping tool.

After *binder activation (step 3)* the cross-section is not changing.

During *handling (step 4)* the preform it is relaxing visibly. As a result the angles between the web and the inner respective the outer flange are not rectangular anymore. The angle between the preform and the inner flange of the consolidation tool goes up to 34°. Additionally the inner radius gets bigger, what makes it more difficult to place the preform in the RTM-tool.

During the *consolidation process (step 5)* the preform moved in negative z-direction about 5 mm. This seems reasonable since the consolidation membrane compacts the preform, which is not fixed to the tool, from above.

8. SUMMARY

The application of a regular grid of red dots on the carbon fibers and the measuring process were automated.

It could be shown that the preforming step has the most effect on the elongation of the preform and fiber disorientations. The elongation of the material was not homogeneous across the part. Furthermore it could be proofed that the preform tends to relax to its original state if it is not held in place (e.g. by a suction tool).

The processes of binder activation, locally and consolidation of the whole preform do not have a great influence on the elongation in frame direction.

The theoretical elongation is about 50% higher compared to the measured results. Also the theoretical shear angle is about 66 % greater compared to the measured results. Therefore it can be concluded that the material is not draped as much as expected in the model. Moreover additional material is used to cover the frame. As a consequence it needs to be taken into account when generating the geometry of the plies.

9. OUTLOOK

For future research other processes of the RTM-chain like ultrasonic fine-trimming and resin-injection need be examined as well in order to tell the influences of theses process steps on elongation and angle of the carbon fibers.

The results of shear angles and fiber disorientations can be verified by an eddy current measurement system.

10. REFERENCES

[1] S. Torstrick, F. Dr.-Ing. Kruse and M. Prof. Dr.-Ing. Wiedemann, "EVo: Net Shape RTM Production Line," *Journal of large-scale research facilities, 2, A66,* p. 7, 2016.

[2] Y. Grohmann, F. Zacharias, F. Kruse and M. P. Wiedemann, "Electrical resistance heating - a method for binder activation in CFRP Processing?," Sevilla (Spain), 2014.

[3] S. Rasche, "Untersuchung zum automatischen Markieren von Kohlenstofffasertextilien für die Qalitätskontrolle von Preform-Prozessen," Hamburg, 2013.

[4] F. F. Kruse, M. Linke, H. Friebe and M. Klein, "Estimation of material properties for draping simulations of carbon ans glassfiber textiles using a 3-D optical deformation measurement system," in *International Conference New Material Characterisitcs to cover New Application Needs*, Paris, 2011.